



# HHS Public Access

Author manuscript

*Biomaterials*. Author manuscript; available in PMC 2018 December 01.

Published in final edited form as:

*Biomaterials*. 2017 December ; 149: 1–11. doi:10.1016/j.biomaterials.2017.09.031.

## Active immunotherapy for TNF-mediated inflammation using self-assembled peptide nanofibers

Carolina Mora-Solano<sup>\*2,3</sup>, Yi Wen<sup>\*1,2</sup>, Huifang Han<sup>2</sup>, Jianjun Chen<sup>2</sup>, Anita S. Chong<sup>2</sup>, Michelle L. Miller<sup>3</sup>, Rebecca R. Pompano<sup>4</sup>, and Joel H. Collier<sup>1,2,3,\*\*</sup>

<sup>2</sup>Department of Surgery, University of Chicago, Chicago, Illinois, 60637, United States

<sup>3</sup>Molecular Pathogenesis Program, University of Chicago, Chicago, Illinois, 60637, United States

<sup>4</sup>Department of Chemistry, University of Virginia, Charlottesville, Virginia, 22904, United States

### Abstract

Active immunotherapies raising antibody responses against autologous targets are receiving increasing interest as alternatives to the administration of manufactured antibodies. The challenge in such an approach is generating protective and adjustable levels of therapeutic antibodies while at the same time avoiding strong T cell responses that could lead to autoimmune reactions. Here we demonstrate the design of an active immunotherapy against TNF-mediated inflammation using short synthetic peptides that assemble into supramolecular peptide nanofibers. Immunization with these materials, without additional adjuvants, was able to break B cell tolerance and raise protective antibody responses against autologous TNF in mice. The strength of the anti-TNF antibody response could be tuned by adjusting the epitope content in the nanofibers, and the T-cell response was focused on exogenous and non-autoreactive T-cell epitopes. Immunization with unadjuvanted peptide nanofibers was therapeutic in a lethal model of acute inflammation induced by intraperitoneally delivered lipopolysaccharide, whereas formulations adjuvanted with CpG showed comparatively poorer protection that correlated with a more Th1-polarized response. Additionally, immunization with peptide nanofibers did not diminish the ability of mice to clear

<sup>\*\*</sup>Corresponding Author. Joel H. Collier, Ph.D., Associate Professor, Biomedical Engineering, Duke University, 101 Science Drive, Campus Box 90281, joel.collier@duke.edu, T: 919-681-9768, F: 919-684-4488.

<sup>†</sup>Current Address: Department of Biomedical Engineering, Duke University, Durham, North Carolina, 27708, United States

<sup>\*</sup>equal contributions

**Publisher's Disclaimer:** This is a PDF file of an unedited manuscript that has been accepted for publication. As a service to our customers we are providing this early version of the manuscript. The manuscript will undergo copyediting, typesetting, and review of the resulting proof before it is published in its final citable form. Please note that during the production process errors may be discovered which could affect the content, and all legal disclaimers that apply to the journal pertain.

### AUTHOR CONTRIBUTIONS

CMS: conducted experiments, analyzed data, wrote manuscript

YW: conducted experiments, analyzed data, wrote manuscript

HH: conducted experiments

JJC: contributed to concept generation, analyzed data

ASC: contributed to concept generation, provided suggestions, reviewed manuscript

MM: conducted experiments, analyzed data

RRP: contributed to concept generation, conducted experiments, analyzed data

JHC: contributed to concept generation, directed the research, analyzed data, wrote manuscript

**Competing Financial Interests.** JHC is an inventor on United States patent US 20120282292 A1, "Methods and compositions related to immunogenic fibrils", assigned to the University of Chicago.

infections of *Listeria monocytogenes*. Collectively this work suggests that synthetic self-assembled peptides can be attractive platforms for active immunotherapies against autologous targets.

### Keywords

Vaccine; supramolecular; adjuvant-free; active immunotherapy; TNF

## INTRODUCTION

Monoclonal antibodies and other biologics have seen explosive growth in the last few decades and now dominate the pharmacological treatment of disease. They have been a tremendous boon to healthcare, and their design, engineering, and manufacturing continue to be advanced, but there remain drawbacks to their use [1]. They are costly to develop, produce, store, and distribute. Many require repeated injections, thereby diminishing patient compliance, and they commonly fail owing to primary unresponsiveness or the induction of antibodies that neutralize the therapeutic molecule and diminish its efficacy over time [2].

A promising but not yet clinically successful way to overcome the disadvantages of monoclonal antibodies is active immunotherapy: stimulating the patient's own immune system to produce therapeutic antibodies against specific problematic self-molecules. This approach has significant potential advantages compared with exogenous antibodies and other biologics, including lower cost, fewer doses required, improved patient compliance, and better tolerance to the treatment. Further, active immunotherapies can raise polyclonal responses, which may have a better capacity to interfere with the target of interest. In the area of active immunotherapy, TNF (tumor necrosis factor) has received particular interest owing to its central role in a variety of chronic inflammatory conditions such as rheumatoid arthritis, psoriasis, and Crohn's disease [3, 4]. Recently, several TNF-directed active immunotherapy strategies have been studied. These include recombinant TNF molecules engineered to contain exogenous CD4<sup>+</sup> T helper epitopes [5, 6], TNF proteins containing unnatural amino acids [7], native TNF conjugated to carrier proteins such as keyhole limpet hemocyanin (KLH) or virus-like particles (VLPs) [8–11], Alum adjuvanted TNF epitope containing carrier proteins [12, 13], and DNA autovaccines against TNF [14]. Currently no active immunotherapy targeting TNF has been clinically approved.

The key objective of active immunotherapy is to raise a predictable and adjustable B cell/ antibody response without an autoreactive T-cell response [4]. This achieves the controllable production of therapeutic antibodies without mounting an autoimmune response against the cells producing the cytokine. To accomplish this, it has been generally believed that three components are necessary: 1) B-cell epitopes from the human target protein [15]; 2) non-autologous T-helper epitopes from a foreign source, incorporated via a carrier protein or by engineering such peptides into a chimeric TNF molecule; and in most cases 3) an adjuvant [16]. For example, TNF-kinoids consist of TNF protein (B-cell epitope source) conjugated to KLH (T-cell epitope source) and formulated with Montanide ISA 51 adjuvant [11, 17].

Peptide vaccines that do not contain any potential TNF T-cell epitopes and only contain TNF B-cell epitopes reduce the likelihood of a T-cell response to native TNF, and so these have

potential safety advantages, but they tend to be poorly immunogenic. TNF B-cell epitope peptides conjugated to carrier proteins have been studied in mice in conjunction with complete Freund's adjuvant (CFA) [18], but this adjuvant is not acceptable for human use. Further, other adjuvants required in most subunit vaccines cause some degree of inflammation, present challenges for regulatory approval, and may not necessarily induce the desired T-helper phenotype and antibody isotypes that are most therapeutic.

Here we report an anti-TNF active immunotherapy that does not require supplemental adjuvants, based on a supramolecular peptide system in which exogenous T-cell epitopes and TNF B-cell epitopes can be co-assembled into long nanofibers with a wide range of possible stoichiometries. This is a departure from peptide-carrier conjugates, which contain only a fixed number of T-cell epitopes and only have room for a limited number of B-cell epitope peptides to be conjugated. More importantly, the peptide nanofibers that the strategy is based on have been previously shown to be remarkably non-inflammatory [19], and they raise strong B-cell and T-cell responses without supplemental adjuvants [19–21]. Other recent work also found in a similar fibrillizing peptide vaccine against *S. aureus* that the relative ratio of B-cell epitopes and T-cell epitopes in the materials had a strong influence on the strength and phenotype of the subsequent immune response [20]. Investigation of a wide range of epitope combinations is enabled by the non-covalent modular construction the materials, which makes it straightforward to economically generate a set of nanofibers with widely varying formulations [20, 22]. In the work reported here, this control over epitope ratio was exploited to adjust the titer of anti-TNF antibodies and select promising formulations for evaluation in animal models of inflammation. In mice, these unadjuvanted peptide nanofibers protected against an otherwise lethal intraperitoneal injection of lipopolysaccharide (LPS), which induces massive TNF-mediated inflammation, but immunizations did not diminish the mice's ability to clear infections of *Listeria monocytogenes*. When these materials were adjuvanted with CpG, this protective effect was compromised, corresponding to a more Th1-polarized response compared to the unadjuvanted and protective nanofibers. Collectively, these results indicated that unadjuvanted supramolecular systems such as the one reported here represent attractive new platforms for development as active immunotherapies.

## MATERIALS AND METHODS

### Peptide Synthesis

TNF<sub>4-23</sub> (SSQNSSDKPVAHVVANHQVE), PADRE (aKXVAAWTLKAa, where X = cyclohexylalanine; a = D-Ala), and Vaccinia IIL<sub>7-21</sub> (QLVFNSISARALKAY) were synthesized in tandem with a (Ser-Gly)<sub>2</sub> linker repeat and the fibrillizing domain of Q11 (epitope-SGSGQQKFQFQFEQQ). Full peptide sequences are shown in the Supplemental Data (Table S1). All peptides were synthesized using standard Fmoc-based chemistry, purified by semi-preparative HPLC, and verified by MALDI [23]. A scrambled version of TNF<sub>4-23</sub> (SKHVNVDNESHVPSQAAVQ) conjugated to Q11 was designed and synthesized to test epitope specific immune responses of peptide nanofibers. Biotinylated peptide epitopes were synthesized for use in ELISA, as reported previously [24].

## Preparation of Immunization Formulations

Unless otherwise indicated, a typical immunization contained TNFQ11 (B-cell epitope), PADREQ11 or VACQ11 T-cell epitope, and unmodified Q11 at a total peptide concentration of 2 mM in PBS. TNFQ11 concentration was 1 mM or 0.2 mM. The concentration of PADREQ11 was titrated from 0.002 mM (0.1 mol % of total peptide) to 0.75 mM (37.5 mol %), and the concentration of VACQ11 in the nanofibers was adjusted from 0.002 mM to 1.25 mM. To prepare formulations for immunizations, dry lyophilized peptides were intermixed by vortexing for 30 min, and then dissolved in sterile water at a total concentration of 8 mM. For formulations with low T-cell epitope concentrations, T-cell epitope-bearing peptides were weighed and dissolved in water at 4× the final concentration, which was then used to dissolve the premixed TNFQ11 and Q11. The peptides were equilibrated overnight at 4 °C. Peptide solutions were then diluted with sterile water and 10× concentrated PBS to a final concentration of 2 mM in 1× PBS, and incubated for at least 3 h at room temperature. This procedure has been previously shown to produce intermixed nanofibers [25]. In some groups, TNFQ11 was replaced with the scrambled TNFQ11 control peptide. CpG-adjuvanted groups contained 10 µg CpG (ODN 1826) per immunization. Formulations adjuvanted with complete Freund's adjuvant (CFA) were emulsified 1:1 in CFA. Endotoxin measurements were conducted on all immunizing formulations using the Limulus Amebocyte Lysate (LAL) kit (Lonza) as described previously [20]. All solutions contained less than 0.5 endotoxin units (EU) per mL, within acceptable limits for mouse studies [26].

## Transmission Electron Microscopy (TEM)

Peptide formulations were diluted to 0.2 mM total peptide in PBS and vigorously vortexed. Five microliters of 0.2 mM peptide nanofibers was deposited onto Formvar/carbon coated 400 mesh copper grids (Electron Microscopy Sciences), washed, stained with 1% w/v uranyl acetate in water, and dried. Samples were imaged on an FEI Tecnai Spirit TEM.

## Mice and Immunizations

Female, wild-type C57BL/6 mice (MHC class II haplotype: I-A<sup>b</sup>) were purchased from Harlan-Envigo laboratories or Charles River laboratories. Animal experiments were approved by the Institutional Animal Care and Use Committees of Duke University and the University of Chicago for work at each respective location. All procedures were in compliance with the NIH Guide for the Care and Use of Laboratory Animals. Mice 8–12 weeks old were used for experiments. Investigators were not blinded or randomized as all samples collected were analyzed or characterized quantitatively. Mice were anesthetized and immunized with 100 µL (200 nmol total peptide) nanofiber formulations subcutaneously (50 µL each at the left and right flank). Two booster immunizations were performed on week 4 and 8, with half doses (100 nmol total peptide), except in one LPS challenge study involving the PADRE formulation 1 and PADRE formulation 2 (Figure 5), booster immunizations were done on week 4 and 16.

### Anti-TNF antibody ELISA

Sera collected from the submandibular vein at designated time points were analyzed for antibody titers by ELISA. Briefly, plates were coated with 1 µg/mL streptavidin in PBS overnight at 4 °C, washed, and then coated with 20 µg/mL biotinylated peptide epitopes (TNF) in PBS. Alternatively, plates were coated with 20 µg/mL TNFQ11 in PBS. In our experiences, these two coating methods produce comparable antibody titers. To detect TNF-specific antibodies, recombinant mouse or human TNF cytokine (Peprotech) was coated at 1 µg/mL in PBS (50 µL each well). Plates were washed with PBS containing 0.05% Tween 20 (PBST) and then blocked with PBST containing 1% bovine serum albumin (PBST-BSA) for 1h at room temperature. Serum was serially diluted PBST-BSA in 10-fold steps from 1:10<sup>1</sup> to 1:10<sup>6</sup>, applied to coated wells, and incubated for 2 h at room temperature. To detect total IgG, HRP conjugated Fcγ fragment specific goat anti-mouse IgG (Jackson Immunoresearch) was used as the detection antibody. For antibody isotyping, HRP-conjugated IgG subtype-specific, i.e. IgG1, IgG2b, IgG2c and IgG3, antibodies were utilized (Southern Biotech). A titer was defined as the highest dilution that produced an absorbance signal higher than the mean + 3\*SD of naive mouse serum. “ND” refers to serum samples with absorbance indistinguishable from pre-immune serum at 1:100 dilution and were categorically given a titer value of 1, to indicate the lack of a measurable titer.

### T Cell ELISPOT

One week after final boost, brachial, axillary, and inguinal draining lymph nodes were collected. Single cell suspensions were prepared and plated at  $0.5 \times 10^6$  cell per well (200 µL) in a 96 well plate (Millipore) pre-coated with anti-mouse IL-4 and IFN-γ capture antibodies (BD Bioscience). Cells were stimulated with TNF peptide (5 µM), PADRE peptide (1µM) or VAC peptide (1µM). Phytohemagglutinin (PHA, 10 µg/mL) or purified hamster anti-mouse CD3 antibodies (clone: 145-2C11, University of Chicago) were utilized as positive controls. Cells were stimulated in a CO<sub>2</sub> incubator at 37°C for 48h. To detect IL-4 and IFN-γ secreting cell spots, biotinylated anti-mouse IL-4 and IFN-γ detection antibody pairs, HRP-streptavidin, and AEC substrate set were used sequentially following the manufacturer’s general guidelines and concentrations (BD Biosciences). Plates were imaged and counted on an ImmunoSpot Analyzer (Cellular Technology, Ltd.). Graphs depict calculated number of spots per 250,000 cells.

### Intraperitoneal LPS Challenge

To induce acute inflammation, mice were challenged with 1 mg/mL lipopolysaccharide (LPS, serotype 055:B5) from *E. coli* (Sigma) in sterile PBS intraperitoneally at a dose of 10 mg/kg one week after the final booster immunization. The mice were monitored for 72 h. Body temperature and body weight were recorded. Humane endpoints were set at: 1) >20% weight loss, 2) significant hypothermia (rectal temperatures below 32 °C) [27], or 3) inability to ambulate, drink, and eat. Immediately before euthanasia, blood was collected for analyzing serum concentrations of TNF cytokine.

## Listeria Infection

Immunized mice were challenged one week after the last boost with  $10^5$  colony-forming units (CFU) of *Listeria monocytogenes* (*Lm*-GFP strain) (200  $\mu$ L) by intraperitoneal injection. Negative controls included mice immunized with sterile PBS and mice immunized with the nanofibers lacking a T-cell epitope. Mice receiving a therapeutic TNF-neutralizing monoclonal antibody (500  $\mu$ g, clone MP6-XT22, Biolegend) 3 hours before *Listeria monocytogenes* challenge were employed as the positive control. The spleen and liver were harvested 48h later. The organs were placed in 5 mL sterile 0.05% Tween-20 in water, diced with scissors, and homogenized with a Tissue Tearor hand held homogenizer (Biospec Products). The homogenized sample (5 mL for the spleen or 6 mL for the liver) was serially diluted 3 times at 1:10 dilution in sterile 0.05% Tween-20 in water. 100  $\mu$ L (spleen) or 120  $\mu$ L (liver) of undiluted, 10-, 100-, and 1000-fold diluted solutions were plated on Brain-Heart Infusion Agar (BD Biosciences) in quadrant-divided Petri dishes. The plates were allowed to air dry inside a sterile hood, then incubated upside down for up to 48 h in a 37°C incubator. The off-white *Listeria* colonies were counted and the total CFU per organ were calculated using the formula: Total CFU= CFU count  $\times$  dilution factor  $\times$  50 (corrected for total organ homogenate volume).

## Surface Plasmon Resonance (SPR)

To assess the quality of serum antibodies raised by peptide assemblies, dissociation rates were measured using a BioRad ProteOn XPR36 Protein Interaction System. To bind TNF, a ProteOn HTG sensor chip (BioRad) with capability to capture His-tagged proteins was conditioned and pre-activated following the manufacturer's instructions. Next, His-tagged recombinant mouse TNF (Genscript) was diluted to 100 nM in PBST and flowed through the vertical lanes of the chip at a rate of 25  $\mu$ L/ min for 5 min. PBST-BSA was then run through the horizontal lanes of the chip at a rate of 25  $\mu$ L/ min for 2 min to reduce non-specific adsorption. Serum samples (n= 10 for TNFQ11/VACQ11/Q11 immunization, n=5 naive serum, n=5 CFA-adjuvanted TNFQ11/VACQ11/Q11 serum) were collected 1 week after the second booster immunization and stored at  $-80^{\circ}\text{C}$  before experiments. Prior to each run, samples were diluted five-fold in PBST-BSA buffer. Antisera were compared with 100  $\mu$ M anti-TNF (clone MP6-XT22) antibody, blank PBST buffer, and pre-immune sera. The non-specific background signal of pre-immune sera was subtracted from the signals of sera samples and anti-TNF antibody. To measure antibody binding affinity to the recombinant TNF on the chip, samples and controls were flowed horizontally at a flow rate of 25  $\mu$ L/min for 5 min. After that, running buffer was flowed over the horizontal lanes of the chip at a rate of 25  $\mu$ L/min for 30 minutes. Absorption and desorption raw data were plotted and fit using KaleidaGraph Software (Synergy).

## Statistical Analysis

Sample sizes and replicates are stated in the figure legends. For LPS challenge experiments (Figure 5), sample sizes and replicates are described in Table S2. Error bars represent means  $\pm$  standard deviations, and data points represent individual mice unless otherwise noted. ANOVA with Tukey's post hoc comparisons or two-sided Student's t-tests were considered more appropriate than non-parametric group comparisons, and were employed as indicated



in the figure legends, with the exception of the survival experiments, which were analyzed using log-rank tests. Sample sizes were chosen based on previous similar studies [20, 24, 28] or pilot experiments preceding the reported experiments. Mice were age-matched as appropriate for each experiment. No additional blinding or randomization was required for the animal studies. Analyses were performed using GraphPad Prism software.

## RESULTS

### Self-assembling nanofibers induce anti-TNF antibodies

Self-assembled nanofibers employed the Q11 fibrillizing sequence for both TNF-derived and exogenous T cell epitopes [19–21, 28–30]. Epitope-bearing peptides were synthesized with Q11 at the C-terminus and the epitope at the N-terminus (sequences in Table S1, assembly schematic in Figure 1f). The peptide TNFQ11 contained an N-terminal B-cell epitope from mouse TNF, residues 4–23 (SSQNSSDKPVAHVVANHQVE). The N-terminal portion, SSQNSSDKP, is located on the surface of soluble TNF [9]. It was predicted to be a linear epitope by BepiPred linear epitope prediction [31]. In addition, there is a flexible -SGSG-linker between the B cell epitope and self-assembling domain Q11. Collectively, these features were anticipated to maintain the immunogenicity of the TNF linear B cell epitope upon fibrillization. This epitope was selected owing to its previously reported ability to raise IgG antibodies that react specifically against the soluble form of TNF but that only weakly bind to the membrane-bound form of TNF [8, 9], contrasting with biologicals that bind both membrane-bound and soluble TNF [2]. This choice was made to maximize the production of neutralizing antibodies against the circulating cytokine while minimizing chances for autoimmunity. It is thought that antibodies raised against this B-cell epitope are capable of binding soluble TNF monomers and disrupting trimer formation, a process required for TNF activity [8, 9]. This B-cell epitope/Q11 peptide was co-assembled with peptides PADREQ11 or VACQ11, which contain an N-terminal CD4<sup>+</sup> T-cell epitope, either the synthetic pan-DR epitope PADRE [32], or I1L<sub>7–21</sub> (VAC), an I-A(b) restricted epitope from Vaccinia I1L protein [33]. PADRE was selected owing to its broad reactivity [32] and also because we have previously had success co-assembling it with B-cell epitopes in other fibrillar peptide assemblies [20]. VAC was additionally investigated in order to increase the likelihood of identifying a suitable T-cell epitope peptide [33].

Q11-based peptides bearing a wide range of N-terminal epitopes have been shown repeatedly to be able to stoichiometrically assemble into integrated nanofibers of controlled composition [20, 22, 24, 25, 28]. Here, in physiological buffers, all three epitope-bearing peptides self-assembled to form nanofibers individually, in binary mixtures with unmodified Q11, and in ternary mixtures of TNFQ11, Q11, and PADREQ11 or VACQ11 (Figure 1, TEM images in a–e, schematic in f). We have previously demonstrated that a key material attribute governing nanofiber internalization by both DCs and macrophages is negative surface charge [19, 24], which had a much larger influence over nanofiber uptake and presentation than other nanofiber properties such as hydrophilicity/hydrophobicity. Because the TNF, PADRE, and VAC epitopes do not possess many negative residues (Table S1), we do not expect the uptake of the nanofiber formulations studied here to be strongly influenced or compromised, despite minor differences in lateral association observed.

In co-assembled peptide nanofibers, simple adjustment of the relative ratios of the T-cell epitope and B-cell epitope has been used previously to vary the resultant antibody titer and the phenotype of the T-cell response [20]. Here we hypothesized that nanofibers incorporating foreign universal T-cell epitopes would provide the necessary T cell help required while the repetitive presentation of TNF B cell epitopes would serve to break B cell tolerance but not T cell tolerance to native TNF [34]. Indeed, mice immunized with nanofibers containing TNFQ11 and either PADREQ11 or VACQ11 raised antibody titers (Figure 2a and 2c, respectively) that bound TNFQ11, the TNF<sub>4-23</sub> peptide epitope, whole mouse TNF, and whole human TNF (Figure 2 and Figure S1). The cross-species reactivity of the antisera is likely owing to the fact that the central SDKPVAHVVAN region of the epitope is conserved across many mammals, including mice, rats, macaques, and humans. Surface plasmon resonance indicated that the antibodies raised against TNF in the VACQ11 system had average  $K_{\text{off}}$  rates of  $7.89 \times 10^{-5}$ , similar to those of an anti-TNF monoclonal antibody ( $4.97 \times 10^{-5}$ ), and slower than the  $K_{\text{off}}$  rates for CFA-adjuvanted formulations ( $1.32 \times 10^{-4}$ ) (Figure S2). In contrast, no detectable antibodies were raised against PADRE (Figure 2b), and weak titers were raised against VAC (Figure 2d), indicating that the VAC T-cell epitope may also have weak B-cell epitope activity. Nanofibers lacking T-cell epitopes failed to raise antibodies at all (Figures 2a and 2c). Further, these responses were lost when a scrambled version of TNF<sub>4-23</sub> was used as the B-cell epitope (Figure S3a). These results indicated that nanofibers co-presenting both self-derived B-cell epitopes and foreign T-cell epitopes can overcome B cell tolerance and raise specific antibody titers against TNF without the use of supplemental adjuvants.

### Anti-TNF antibody responses were adjustable by titrating the T-cell epitope content

We expected that titrating the amount of PADREQ11 or VACQ11 in the nanofibers relative to the amount of TNF B-cell epitopes would influence the strength of the antibody response, based on previous observations of similar nanofibers formulated for a *S. aureus* vaccine [20]. To test this, we prepared nanofibers that contained 50% of the B-cell epitope (TNFQ11) and the balance of a variable mixture of PADREQ11 and unmodified Q11. The three peptides were mixed as dry powders prior to self-assembly in a process shown previously to produce mixed peptide fibrils [20, 25]. The formulated nanofibers contained as little as 0.002mM (0.1%) PADREQ11 and as much as 0.75mM (37.5%) PADREQ11, a range spanning a several hundred-fold difference in concentration. As PADREQ11 was titrated into the nanofibers, it progressively improved TNF-specific IgG titers up to formulations containing 0.05mM (2.5%) PADREQ11. Interestingly, increasing the PADREQ11 content beyond this diminished the antibody responses (Figure 3a). These results are consistent with the previous *S. aureus* vaccination study that employed nanofibers containing PADREQ11 [20], which also showed similar maximum responses at intermediate levels of PADRE incorporation. To determine whether this bell-shaped curve is specific to PADRE or may be more generalizable to other T-cell epitopes, we investigated a second CD4<sup>+</sup> T helper epitope from Vaccinia virus (QLVFNSISARALKAY, VAC). This epitope had not been tested before in peptide nanofiber formulations. We tested VACQ11 concentrations from 0.002mM (0.1 mol % in nanofibers) up to 1.25mM (50 mol% in nanofibers). Antibody responses progressively improved with increasing VACQ11, with no clear optimum within the range tested, contrary to PADREQ11 (Figure 3c). To test if there were any differences in the quality of the



antibodies, we investigated the IgG subclasses raised by nanofibers containing each T-cell epitope. Formulations with both T-cell epitopes elicited a combination of IgG1, IgG2b, IgG2c, and IgG3 antibodies, but PADREQ11 appeared to favor IgG1 to a greater extent than VACQ11, which elicited IgG1, IgG2b, IgG2c, and IgG3 at more similar levels (Figure3b and 3d). These results demonstrated a simple method, adjusting the T-cell epitope content in the nanofibers, to tune the quantity and quality of anti-TNF antibodies.

### **Cell-mediated immunity depended on T-cell epitope concentration and was focused on exogenous T-cell epitopes**

A significant potential limitation of active immunization strategies for blocking TNF-mediated inflammation is the possibility of inducing cell-mediated immunity against TNF-expressing cells, as TNF has important functions in host defense and secondary lymphoid organization, and cell-mediated immunity could lead to increased levels of inflammation, tissue damage, immunosuppression, or potential autoimmunity [35]. We hypothesized that using a foreign T-cell epitope (PADRE or VAC) would minimize T-cell responses to endogenous targets yet still facilitate therapeutic antibody titers specifically against the desired B-cell epitope of TNF. To test this, we collected draining lymph node cells from immunized mice and investigated how T-cell epitope dose influenced the strength and polarization of the T-cell response using ELISPOT for IL-4 and IFN $\gamma$  production. T-cell responses to PADRE depended on the dose of the T-cell epitope, in a similar manner to the dose-responsiveness of the antibody titers (Figure4a and 4b). T-cell responses to PADRE were also IL-4-dominant, with considerably more IL-4-secreting cells than IFN $\gamma$ -secreting cells (Figure4a and 4b). Furthermore, we found that the doses that most stimulated B cell/antibody responses did not correspond with those eliciting the strongest T-cell responses, and specific formulations were capable of abolishing the T-cell response altogether. The highest antibody response was produced at 0.05mM PADREQ11, whereas the highest T-cell response was produced at 0.002 mM PADREQ11 and diminished with increasing PADREQ11. At the optimal formulation for anti-TNF antibody responses (0.05 mM), fewer than 5 cells per million produced IL-4 in response to TNF peptide (Figure 4a), and at 0.75 mM PADREQ11, there was no T-cell response to either PADRE or the TNF B-cell epitope (Figure4a and 4b).

T-cell responses to VAC nanofibers were more balanced between IL-4 and IFN $\gamma$  (Figure4c and 4d). Additionally, the amount of VAC T-cell epitope necessary for eliciting maximal T-cell responses was also different than the amount eliciting maximal antibody responses, with 0.05 mM eliciting maximal T-cell responses (both IL-4 and IFN $\gamma$ ) and 1.25 mM eliciting maximal antibody titers. Thus, by creating a range of nanofibers with varying epitope contents, different combinations of T-cell responses and antibody responses could be generated, and from these options specific attractive formulations can be selected for advancement into further development. Moving forward, we selected combinations of antibody and T-cell responses most likely to produce neutralizing anti-TNF antibodies without significant Th1/Th2 cell responses against the TNF-derived B-cell epitope.

## Immunization protected from TNF-mediated inflammation in mice

In a model of TNF-mediated inflammation, prior immunization with peptide nanofibers provided significant protection (Figure 5). We used a model in which intraperitoneally delivered lipopolysaccharide (LPS) induces shock-like symptoms, including weight loss and hypothermia [36–39]. Without immunization, this model was lethal for 77–100% of mice in control groups, with mice removed from the study upon reaching predetermined cutoffs (20% body weight loss or 32 °C body temperature, Figure 5a). Strikingly, immunizations with either nanofibers containing TNFQ11/PADREQ11 or TNFQ11/VACQ11 resulted in markedly improved survival (Figure 5a–b). Complete protection was provided by a formulation of 0.2 mM TNFQ11/0.05 mM PADREQ11/1.75 mM Q11 (PADRE formulation 2, Group B in Figure 5a–b). Notably, protection experiments were performed in two different locations (Univ. Chicago and Duke University), in different animal facilities, and by different researchers (CMS at Chicago and YW at Duke), indicating the robustness of the finding (description of experimental groups in Table S2). 90% protection was afforded by two other formulations: 1 mM TNFQ11/0.05 mM PADREQ11/0.95 mM Q11 (PADRE formulation 1, Group A in Figure 5a–b) and 1 mM TNFQ11/1.25 mM VACQ11/0.25 mM Q11 (VAC formulation, Group C in Figure 5a–b). In contrast, formulations lacking T-cell epitopes (Group E) conferred no protection. Separately we also investigated vaccinations containing scrambled B-cell epitopes, which likewise were not protective (Figure S3). Anti-TNF titers remained consistent before and after LPS challenge, indicating that the increased production of TNF during the experiment did not have a booster effect on the nanofiber immunization (Figure S6). Circulating TNF values were also measured at the time of sacrifice, showing that all mice receiving LPS had elevated circulating TNF (Figure S7), whereas recovering mice returned their TNF levels to baseline by 72 h. A plausible explanation for the presence of elevated TNF in both surviving mice and those that succumbed could be that the antibodies raised by the immunizations neutralized TNF yet did not promote its rapid clearance on the time scale of the LPS experiment. Such neutralized but still-circulating TNF would be detectable if the ELISA antibody bound sites on TNF different from the antibodies raised by immunization. Finally, we investigated nanofiber formulations adjuvanted with CpG. These elicited titers of anti-TNF antibodies higher than unadjuvanted formulations (Figure S8), yet unexpectedly mice were only partially protected, with only 40% surviving the LPS challenge (Figure 5b), a marked diminishment compared to the unadjuvanted immunizations. This result indicated that antibody titers are not the only requirement for protection and that other factors influencing the phenotype of the immune response could impact the therapeutic efficacy. In this regard, the unadjuvanted nature of peptide nanofibers may have advantages over formulations requiring adjuvants. To explore these phenotypic considerations further, we compared the Th1/Th2 bias between unadjuvanted formulations and those containing CpG, finding that unadjuvanted TNFQ11/VACQ11 produced an overall Th2-biased T-cell response, whereas the addition of CpG biased the response toward Th1 (Figure 5c–d). Compared with the prior investigation of IL-4 and IFN $\gamma$  shown in Figure 4, which showed a relatively non-polarized Th1/Th2 phenotype for unadjuvanted VACQ11 nanofibers, the response was found to be more Th2-polarized upon further investigation here. Previous investigations of Q11-based materials using other epitopes such as ovalbumin have found similar variability, where T-cell responses can be at times unpolarized [19] or Th2-slanted [20], but not Th1-slanted. It is not presently well

understood what parameters specify the range of T-cell phenotypes for fibrillized peptide nanofiber vaccines, nor what contributes to differences in T-cell phenotypes observed *in vivo* or *ex vivo*. Further study will be required to ascertain these relationships and to determine whether a causal relationship exists between Th2 phenotypes and the protective ability of peptide nanofiber immunizations. Currently, the correlation is notable.

### **The ability to clear infections was not impaired by peptide nanofiber immunization**

We hypothesized that immunization with TNF/VAC nanofibers would not diminish the ability to clear infections because the B-cell epitope chosen was previously found to raise antibodies against soluble TNF, not transmembrane TNF [9]. An inadvertent targeting of transmembrane TNF, which is expressed on activated macrophages, lymphocytes, and other cells, could lead to destruction of these cells and an impaired ability to respond to infection. Indeed, mice receiving an anti-TNF monoclonal antibody 3 hours ahead that were then challenged intraperitoneally with  $1 \times 10^5$  CFU of *Listeria* showed elevated CFUs in their livers and spleens 48 hours later (Figure 6a). In contrast, mice immunized with TNFQ11/VACQ11 showed CFUs indistinguishable from unimmunized mice or those that had received non-functional nanofibers lacking the VAC T-cell epitope (Figure 6b). These findings indicated that TNF/VAC nanofibers did not diminish the ability of the animals to control *Listeria* infections, even when they raised anti-TNF antibodies.

## **DISCUSSION**

Supramolecular peptide materials may be suitable for development as active immunotherapies against autologous targets, a departure from previously described uses of these materials that have focused primarily on their use as scaffolds for cell culture and delivery or as vaccines against cancer or infectious diseases [40–42]. Platforms that share structural similarities with Q11 and which may be interesting to study in this regard include other peptides that form into long, high-aspect ratio nanofibers. For example the peptide KFE8 has been explored previously in vaccinations against cocaine addiction [43]; the peptide RADA4 has been explored as a depot-forming material in vaccines against hepatitis B [44]; the peptide EAK16 has been investigated in vaccines against HIV [45]; the peptide Ac-AAVLLLLW-COOH has been explored in anticancer vaccines [46]; and Q11 has been explored in applications including malaria [47], influenza [19], *S. aureus* vaccines [20], and cancer [48]. Other fibrous self-assemblies include those composed of peptide amphiphiles, which have been explored in anticancer vaccines [49] and vaccines against group A streptococcus [50]. Despite the range of infectious diseases that peptide assemblies have already been developed toward, this still represents a small portion of the current breadth of application for peptide self-assemblies overall, which further includes 3D cell culture, matrices for regenerative medicine, and the controlled release or delivery of cells and therapeutics [40, 51]. Because these materials share structural similarities, it may be useful to determine whether they represent, as a class, advantageous platforms for active immunotherapy against autologous targets.

Advantages that supramolecular assemblies appear to have is that they are noninflammatory [19]. Therefore, it is unlikely that anti-TNF nanofibers would trigger the production of

proinflammatory cytokines. In addition, they do not require supplemental adjuvants, and they do not strongly engage Th1-type T-cell responses [19, 52], which correlates with their good performance in the mouse model studied here. Another advantage is the modularity of the system, which allows the adjustment of the epitope content within the material simply by mixing different amounts of component peptides prior to fibrillization. In the results reported here, this adjustment influenced the titer of antibodies raised, as well as the strength of Th1 and Th2 T-cell responses to the PADRE or VAC CD4<sup>+</sup> T-cell epitopes. It was straightforward to compare formulations containing different ratios between T-cell epitopes and B-cell epitopes, from as low as 1:500 to beyond 1:1. It would be comparatively more difficult to adjust the epitope ratio and content widely within other systems such as carrier proteins, engineered conjugates, or kinoids, because such steps commonly require cloning or an individually optimized conjugation reaction for each particular formulation, and such platforms have fewer sites for inserting or attaching various epitopes to achieve wide ranges in their relative ratios. Nanofibers containing variable amounts of VAC or PADRE produced unique dose-response curves for antibody and T-cell responses (Figures 3 and 4). It is possible that these distinctive responses arise from the different affinities of each peptide for MHC class-II molecules or differences in the affinities of T-cell receptors for each peptide-MHC complex, as both have been found to influence T-cell phenotype [53–56]. For both epitopes the formulations generating the greatest antibody responses did not match those generating the strongest effector T-cell responses (Figures 3 and 4). For the PADRE T-helper epitope, antibody responses were greatest at 0.05 mM peptide, whereas T-cell responses were greatest at 0.002 mM PADRE. For the VAC T-helper epitope, antibody responses were greatest at 1.25 mM peptide (the highest dose tested) whereas T-cell responses were greatest at 0.05 mM. Another previously investigated series of T/B epitope combinations in a Q11-based vaccine against methicillin-resistant *Staphylococcus aureus* (MRSA) likewise exhibited a strong dose-response curve, with different formulations favoring antibody or T-effector responses [20]. Together these studies indicate that peptide assembly can be utilized to efficiently generate a series of different epitope ratios, and these can be selected for preferred combinations of T- and B-cell responses. Although it is unclear why the highest PADRE doses led to diminished antibody responses, possible causes include masking of the B cell epitope on the nanofiber, a reduction in T<sub>FH</sub> cells, or an increase in Tregs. Previous studies have supported the concept that antigen dose influences the differentiation of CD4 Th1/Th2/T<sub>FH</sub> phenotypes [53, 57, 58]. High antigen dose can also increase the amount of peptide:MHC class II molecules displayed on antigen-presenting cells, thereby increasing TCR signaling strength and duration towards specific T cells [54]. Whereas low antigen doses have been reported to favor Th1 differentiation, intermediate-to-high antigen doses induced Th2-dominated responses in a T cell receptor- $\alpha\beta$ -transgenic model [58]. Antigen dose or recognition of pMHC by high affinity TCRs has also been observed to modulate T<sub>FH</sub> cell differentiation [53, 57]. We also observed formulations for which antibody or T-cell responses were greatly reduced or abolished, which may ultimately be useful for eliciting antigen-specific T- or B-cell tolerance against autoimmune epitopes or allergens. Because such effects are difficult to predict for different epitope systems and under different adjuvating conditions in different groups, simple access to a range of different epitope combinations in co-assembled peptide nanofibers provides a straightforward empirical platform for surveying different formulations and selecting candidates for further

development. In addition, it will be interesting to examine how nanofiber attributes affect B cell activation in the germinal center in the future. The production of various antibody isotypes indicates that B-cell activation has occurred, accompanied by gene recombination and somatic hypermutation, but the full mechanism of adjuvancy of Q11 nanofibers continues to be investigated. Additionally, size, stability, lateral association, and surface charge are several parameters that would be advantageous to study in further detail. The stability of the nanofibers to degradation or disassembly would be particularly interesting to study, as we expect the overall stability of the  $\beta$ -sheet structure to be able to provide either a local depot at the injection site or a prolonged presence within lymph nodes or even within APCs. It would likewise be interesting to investigate whether the route of administration (intraperitoneal, intramuscular, intradermal, subcutaneous) influences the phenotype or duration of the immune response observed. Although previous investigations of Q11 nanofibers indicated that similar titers of antibodies were raised by both intraperitoneal and subcutaneous injections [19], subtle phenotypic differences may exist. In any context, there remains considerable investigation to be conducted in the future to optimize the design of nanofiber-based immunotherapies.

In sum, self-assembled peptide nanofibers demonstrate attractive properties for the development of active immunotherapies against autologous targets. They can be formulated to contain exogenous T-cell epitopes, and the facile incorporation of a wide range of B- and T-cell concentrations in the nanofibers can be used to adjust the antibody titers and T-cell responses that are generated. They were therapeutic in an acute model of TNF-mediated inflammation, whereas additional CpG adjuvant unexpectedly diminished protection. The present study provides a strong rationale for the further study of such materials in specific disease models of chronic, acute, or congenital inflammatory conditions.

## Supplementary Material

Refer to Web version on PubMed Central for supplementary material.

## Acknowledgments

This research was supported by the National Institutes of Health (NIBIB 5R01EB009701; NIAID 5R01AI118182; and NIAMS 7R21AR066244). The contents are solely the responsibility of the authors and do not necessarily represent the official views of these agencies. The authors thank Stephen Meredith for assistance with the analysis of SPR data.

## References

1. Hansel TT, Kropshofer H, Singer T, Mitchell JA, George AJT. The safety and side effects of monoclonal antibodies. *Nat Rev Drug Discov.* 2010; 9:325–38. [PubMed: 20305665]
2. Ware, CF. *Advances in Pharmacology.* Webb, DR., editor. Academic Press; 2013. p. 51-80.
3. Zagury D, Le Buanec H, Bizzini B, Burny A, Lewis G, Gallo RC. Active versus passive anti-cytokine antibody therapy against cytokine-associated chronic diseases. *Cytokine Growth Factor Rev.* 2003; 14:123–37. [PubMed: 12651224]
4. Jia T, Pan Y, Li J, Wang L. Strategies for active TNF-alpha vaccination in rheumatoid arthritis treatment. *Vaccine.* 2013; 31:4063–8. [PubMed: 23845805]
5. Dalum I, Butler DM, Jensen MR, Hindersson P, Steinaa L, Waterston AM, et al. Therapeutic antibodies elicited by immunization against TNF-[alpha]. *Nat Biotech.* 1999; 17:666–9.

6. Wan Y, Xue X, Li M, Zhang X, Qin X, Zhang C, et al. Prepared and screened a modified TNF- $\alpha$  molecule as TNF- $\alpha$  autovaccine to treat LPS induced endotoxic shock and TNF- $\alpha$  induced cachexia in mouse. *Cell Immunol.* 2007; 246:55–64. [PubMed: 17592730]
7. Grünewald J, Hunt GS, Dong L, Niessen F, Wen BG, Tsao M-L, et al. Mechanistic studies of the immunochemical termination of self-tolerance with unnatural amino acids. *Proc Natl Acad Sci USA.* 2009; 106:4337–42. [PubMed: 19246393]
8. Chackerian B, Lowy DR, Schiller JT. Conjugation of a self-antigen to papillomavirus-like particles allows for efficient induction of protective autoantibodies. *J Clin Invest.* 2001; 108:415–23. [PubMed: 11489935]
9. Spohn G, Guler R, Johansen P, Keller I, Jacobs M, Beck M, et al. A Virus-Like Particle-Based Vaccine Selectively Targeting Soluble TNF- Protects from Arthritis without Inducing Reactivation of Latent Tuberculosis. *J Immunol.* 2007; 178:7450–7. [PubMed: 17513796]
10. Le Buanec H, Delavallée L, Bessis N, Paturance S, Bizzini B, Gallo R, et al. TNF $\alpha$  kinoid vaccination-induced neutralizing antibodies to TNF $\alpha$  protect mice from autologous TNF $\alpha$ -driven chronic and acute inflammation. *Proc Natl Acad Sci USA.* 2006; 103:19442–7. [PubMed: 17158801]
11. Durez P, Vandepapeliere P, Miranda P, Toncheva A, Berman A, Kehler T, et al. Therapeutic vaccination with TNF-Kinoid in TNF antagonist-resistant rheumatoid arthritis: a phase II randomized, controlled clinical trial. *PLoS ONE.* 2014; 9:e113465. [PubMed: 25517733]
12. Zhang L, Wang J, Xu A, Zhong C, Lu W, Deng L, et al. A Rationally Designed TNF- $\alpha$  Epitope-Scaffold Immunogen Induces Sustained Antibody Response and Alleviates Collagen-Induced Arthritis in Mice. *PLoS ONE.* 2016; 11:e0163080. [PubMed: 27658047]
13. Bavoso A, Ostuni A, De Vendel J, Bracalello A, Shcheglova T, Makker S, et al. Aldehyde modification and alum coadjuvancy enhance anti-TNF- $\alpha$  autovaccination and mitigate arthritis in rat. *J Pept Sci.* 2015; 21:400–7. [PubMed: 25424319]
14. Wildbaum G, Youssef S, Karin N. A Targeted DNA Vaccine Augments the Natural Immune Response to Self TNF- and Suppresses Ongoing Adjuvant Arthritis. *J Immunol.* 2000; 165:5860–6. [PubMed: 11067946]
15. Goodnow CC, Vinuesa CG, Randall KL, Mackay F, Brink R. Control systems and decision making for antibody production. *Nat Immunol.* 2010; 11:681–8. [PubMed: 20644574]
16. Coffman RL, Sher A, Seder RA. Vaccine adjuvants: putting innate immunity to work. *Immunity.* 2010; 33:492–503. [PubMed: 21029960]
17. Biton J, Semerano L, Delavallee L, Lemeiter D, Laborie M, Grouard-Vogel G, et al. Interplay between TNF and regulatory T cells in a TNF-driven murine model of arthritis. *J Immunol.* 2011; 186:3899–910. [PubMed: 21346237]
18. Capini CJ, Bertin-Maghit SM, Bessis N, Haumont PM, Bernier EM, Muel EG, et al. Active immunization against murine TNF $\alpha$  peptides in mice: generation of endogenous antibodies cross-reacting with the native cytokine and in vivo protection. *Vaccine.* 2004; 22:3144–53. [PubMed: 15297067]
19. Chen J, Pompano RR, Santiago FW, Maillat L, Sciammas R, Sun T, et al. The use of self-adjuvanting nanofiber vaccines to elicit high-affinity B cell responses to peptide antigens without inflammation. *Biomaterials.* 2013; 34:8776–85. [PubMed: 23953841]
20. Pompano RR, Chen J, Verbus EA, Han H, Fridman A, McNeely T, et al. Titrating T-cell epitopes within self-assembled vaccines optimizes CD4+ helper T cell and antibody outputs. *Adv Healthc Mater.* 2014; 3:1898–908. [PubMed: 24923735]
21. Rudra JS, Tian YF, Jung JP, Collier JH. A self-assembling peptide acting as an immune adjuvant. *Proc Natl Acad Sci USA.* 2009; 107:622–7. [PubMed: 20080728]
22. Jung JP, Moyano JV, Collier JH. Multifactorial optimization of endothelial cell growth using modular synthetic extracellular matrices. *Integr Biol.* 2011; 3:185.
23. Jung JP, Nagaraj AK, Fox EK, Rudra JS, Devgun JM, Collier JH. Co-assembling peptides as defined matrices for endothelial cells. *Biomaterials.* 2009; 30:2400–10. [PubMed: 19203790]
24. Wen Y, Waltman A, Han H, Collier JH. Switching the Immunogenicity of Peptide Assemblies Using Surface Properties. *ACS Nano.* 2016; 10:9274–86.



25. Gasiorowski JZ, Collier JH. Directed intermixing in multicomponent self-assembling biomaterials. *Biomacromolecules*. 2011; 12:3549–58. [PubMed: 21863894]
26. Malyala P, Singh M. Endotoxin limits in formulations for preclinical research. *J Pharm Sci*. 2008; 97:2041–4. [PubMed: 17847072]
27. Blanqué R, Meakin C, Millet S, Gardner CR. Hypothermia as an indicator of the acute effects of lipopolysaccharides: comparison with serum levels of IL1 $\beta$ , IL6 and TNF $\alpha$ . *Gen Pharmac*. 1996; 27:973–7.
28. Hudalla GA, Sun T, Gasiorowski JZ, Han H, Tian YF, Chong AS, et al. Graded assembly of multiple proteins into supramolecular nanomaterials. *Nat Mater*. 2014; 13:829–36. [PubMed: 24930032]
29. Hudalla GA, Modica JA, Tian YF, Rudra JS, Chong AS, Sun T, et al. A self-adjuvanting supramolecular vaccine carrying a folded protein antigen. *Adv Healthc Mater*. 2013; 2:1114–9. [PubMed: 23436779]
30. Collier JH, Messersmith PB. Enzymatic Modification of Self-Assembled Peptide Structures with Tissue Transglutaminase. *Bioconjug Chem*. 2003; 14:748–55. [PubMed: 12862427]
31. Larsen JE, Lund O, Nielsen M. Improved method for predicting linear B-cell epitopes. *Immunome Res*. 2006; 2:2. [PubMed: 16635264]
32. Alexander J, Sidney J, Southwood S, Ruppert J, Oseroff C, Maewal A, et al. Development of high potency universal DR-restricted helper epitopes by modification of high affinity DR-blocking peptides. *Immunity*. 1994; 1:751–61. [PubMed: 7895164]
33. Moutaftsi M, Bui HH, Peters B, Sidney J, Salek-Ardakani S, Oseroff C, et al. Vaccinia virus-specific CD4<sup>+</sup> T cell responses target a set of antigens largely distinct from those targeted by CD8<sup>+</sup> T cell responses. *J Immunol*. 2007; 178:6814–20. [PubMed: 17513729]
34. Bachmann MF, Rohrer UH, Kundig TM, Burki K, Hengartner H, Zinkernagel RM. The influence of antigen organization on B cell responsiveness. *Science*. 1993; 262:1448–51. [PubMed: 8248784]
35. Winsauer C, Kruglov AA, Chashchina AA, Drutskaya MS, Nedospasov SA. Cellular sources of pathogenic and protective TNF and experimental strategies based on utilization of TNF humanized mice. *Cytokine Growth Factor Rev*. 2014; 25:115–23. [PubMed: 24405806]
36. Bessede A, Gargaro M, Pallotta MT, Matino D, Servillo G, Brunacci C, et al. Aryl hydrocarbon receptor control of a disease tolerance defence pathway. *Nature*. 2014; 511:184–90. [PubMed: 24930766]
37. Lehmann V, Freudenberg MA, Galanos C. Lethal toxicity of lipopolysaccharide and tumor necrosis factor in normal and D-galactosamine-treated mice. *J Exp Med*. 1987; 165:657–63. [PubMed: 3819645]
38. Juskewitch JE, Knudsen BE, Platt JL, Nath KA, Knutson KL, Brunn GJ, et al. LPS-induced murine systemic inflammation is driven by parenchymal cell activation and exclusively predicted by early MCP-1 plasma levels. *Am J Pathol*. 2012; 180:32–40. [PubMed: 22067909]
39. Tateda K, Matsumoto T, Miyazaki S, Yamaguchi K. Lipopolysaccharide-induced lethality and cytokine production in aged mice. *Infect Immun*. 1996; 64:769–74. [PubMed: 8641780]
40. Webber MJ, Appel EA, Meijer EW, Langer R. Supramolecular biomaterials. *Nat Mater*. 2016; 15:13–26. [PubMed: 26681596]
41. Wen Y, Collier JH. Supramolecular peptide vaccines: tuning adaptive immunity. *Curr Opin Immunol*. 2015; 35:73–9. [PubMed: 26163376]
42. Mora-Solano C, Collier JH. Engaging adaptive immunity with biomaterials. *J Mater Chem B*. 2014; 2:2409–21.
43. Rudra JS, Ding Y, Neelakantan H, Ding C, Appavu R, Stutz S, et al. Suppression of Cocaine-Evoked Hyperactivity by Self-Adjuvanting and Multivalent Peptide Nanofiber Vaccines. *ACS Chem Neurosci*. 2016; 7:546–52. [PubMed: 26926328]
44. Grenfell RF, Shollenberger LM, Samli EF, Harn DA. Vaccine self-assembling immune matrix is a new delivery platform that enhances immune responses to recombinant HBsAg in mice. *Clin Vaccine Immunol*. 2015; 22:336–43. [PubMed: 25609075]
45. Ding Y, Liu J, Lu S, Igweze J, Xu W, Kuang D, et al. Self-assembling peptide for co-delivery of HIV-1 CD8<sup>+</sup> T cells epitope and Toll-like receptor 7/8 agonists R848 to induce maturation of

- monocyte derived dendritic cell and augment polyfunctional cytotoxic T lymphocyte (CTL) response. *J Control Release*. 2016; 236:22–30. [PubMed: 27297778]
46. Rad-Malekshahi M, Fransen MF, Krawczyk M, Mansourian M, Bourajjaj M, Chen J, et al. Self-Assembling Peptide Epitopes as Novel Platform for Anticancer Vaccination. *Mol Pharm*. 2017; 14:1482–93. [PubMed: 28088862]
  47. Rudra JS, Mishra S, Chong AS, Mitchell RA, Nardin EH, Nussenzweig V, et al. Self-assembled peptide nanofibers raising durable antibody responses against a malaria epitope. *Biomaterials*. 2012; 33:6476–84. [PubMed: 22695068]
  48. Huang Z-H, Shi L, Ma J-W, Sun Z-Y, Cai H, Chen Y-X, et al. a Totally Synthetic, Self-Assembling, Adjuvant-Free MUC1 Glycopeptide Vaccine for Cancer Therapy. *J Am Chem Soc*. 2012; 134:8730–3. [PubMed: 22587010]
  49. Black M, Trent A, Kostenko Y, Lee JS, Olive C, Tirrell M. Self-Assembled Peptide Amphiphile Micelles Containing a Cytotoxic T-Cell Epitope Promote a Protective Immune Response In Vivo. *Adv Mater*. 2012; 24:3845–9. [PubMed: 22550019]
  50. Trent A, Ulery BD, Black MJ, Barrett JC, Liang S, Kostenko Y, et al. Peptide Amphiphile Micelles Self-Adjuvant Group A Streptococcal Vaccination. *The AAPS Journal*. 2015; 17:380–8. [PubMed: 25527256]
  51. Acar H, Srivastava S, Chung EJ, Schnorenberg MR, Barrett JC, LaBelle JL, et al. Self-assembling peptide-based building blocks in medical applications. *Adv Drug Deliv Rev*. 2016; 110–111:65–79.
  52. Vigneswaran Y, Han H, De Loera R, Wen Y, Zhang X, Sun T, et al. Peptide biomaterials raising adaptive immune responses in wound healing contexts. *J Biomed Mater Res Part A*. 2016; 104:1853–62.
  53. Keck S, Schmalzer M, Ganter S, Wyss L, Oberle S, Huseby ES, et al. Antigen affinity and antigen dose exert distinct influences on CD4 T-cell differentiation. *Proc Natl Acad Sci USA*. 2014; 111:14852–7. [PubMed: 25267612]
  54. Gottschalk RA, Hathorn MM, Beuneu H, Corse E, Dustin ML, Altan-Bonnet G, et al. Distinct influences of peptide-MHC quality and quantity on in vivo T-cell responses. *Proc Natl Acad Sci USA*. 2012; 109:881–6. [PubMed: 22223661]
  55. Stone JD, Chervin AS, Kranz DM. T-cell receptor binding affinities and kinetics: impact on T-cell activity and specificity. *Immunology*. 2009; 126:165–76. [PubMed: 19125887]
  56. Lever M, Maini PK, van der Merwe PA, Dushek O. Phenotypic models of T cell activation. *Nat Rev Immunol*. 2014; 14:619–29. [PubMed: 25145757]
  57. Fazilleau N, McHeyzer-Williams LJ, Rosen H, McHeyzer-Williams MG. The function of follicular helper T cells is regulated by the strength of T cell antigen receptor binding. *Nat Immunol*. 2009; 10:375–84. [PubMed: 19252493]
  58. Hosken NA, Shibuya K, Heath AW, Murphy KM, O'Garra A. The effect of antigen dose on CD4+ T helper cell phenotype development in a T cell receptor-alpha beta-transgenic model. *J Exp Med*. 1995; 182:1579–84. [PubMed: 7595228]

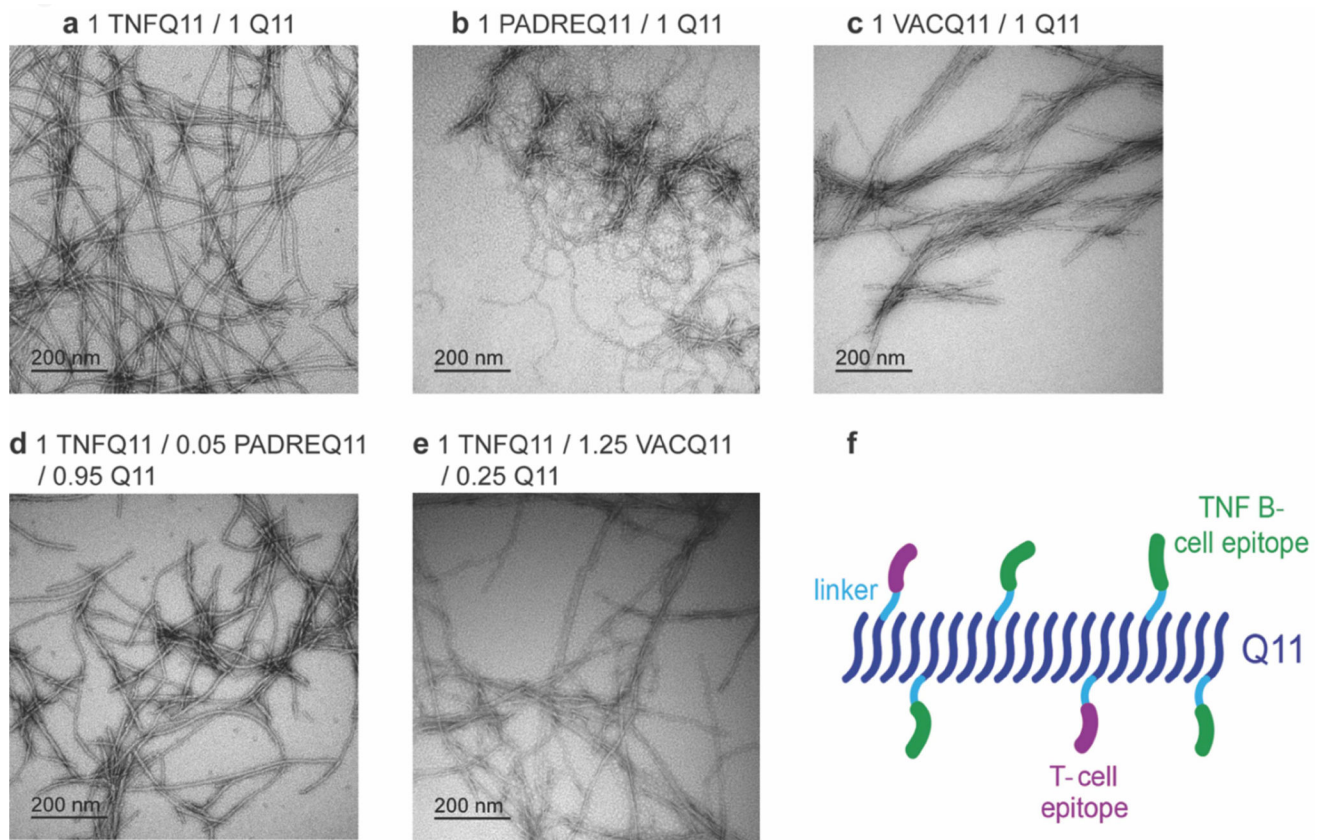


**Fig 1. TEM and schematic of co-assembled peptide nanofibers**

Negative-stained TEM images of nanofibers (prepared at 2 mM total peptide concentration and diluted to 0.2 mM for imaging) (a) TNFQ11/Q11 (1:1 molar ratio), (b) PADREQ11/Q11 (1:1), (c) VACQ11/Q11 (1:1), (d) TNFQ11/PADREQ11/Q11 (1:0.05:0.95), (e) TNFQ11/VACQ11/Q11 (1:1.25:0.25). (f) schematic of co-assembled peptide nanofibers containing B-cell epitopes and T-cell epitopes.

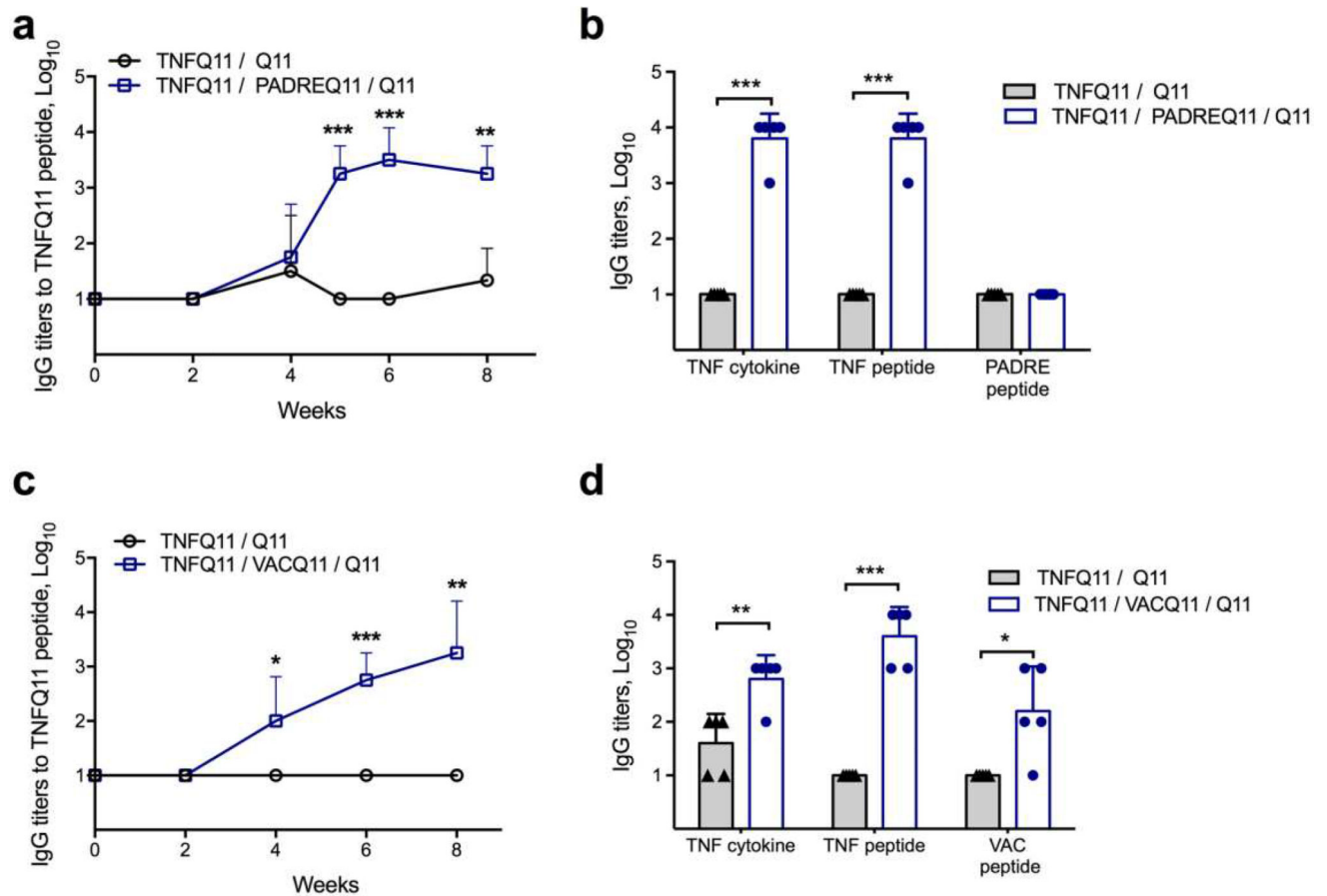


**Fig 2. Co-assembled peptide nanofibers raise anti-TNF antibodies**

(a) TNFQ11 peptide-specific IgG responses in the sera of mice immunized with formulations with or without the self-assembling T-cell epitope PADREQ11, evaluated over time by ELISA. (b) Reactivity of immune sera against TNF cytokine (mouse), TNF<sub>4-23</sub> peptide, and PADRE peptide. (c) TNFQ11 peptide-specific IgG responses in the sera of mice immunized with formulations with or without the self-assembling T-cell epitope VACQ11, evaluated over time by ELISA. (d) Reactivity of immune sera against TNF cytokine, TNF<sub>4-23</sub> peptide, and VAC peptide. Only T-cell epitope-containing assemblies raised significant IgG responses against TNF peptide and TNF cytokine, and there was minimal antibody development against the T-cell epitopes PADRE or VAC. Formulations were 1 mM TNFQ11/0.05 mM PADREQ11/ 0.95 mM Q11 (a–b), 1mM TNFQ11/0.25 mM VACQ11/0.75 mM VACQ11 (c), and 1mM TNFQ11/1.25 mM VACQ11/0.25 mM Q11 (d). In (a, c) mice were immunized at week 0 and boosted at week 4 with a half dose. In (b, d), titers were measured after priming and two boosts at weeks 4 and 8. Mean  $\pm$  SD is shown.  $n=4$  for each group in a and c.  $n=5$  for each group in b and d. Statistical significance was confirmed by t-test at each time point (a and c) or for each antigen (b and d). \*  $p<0.05$ , \*\*  $p<0.01$ , \*\*\*  $p<0.001$ .

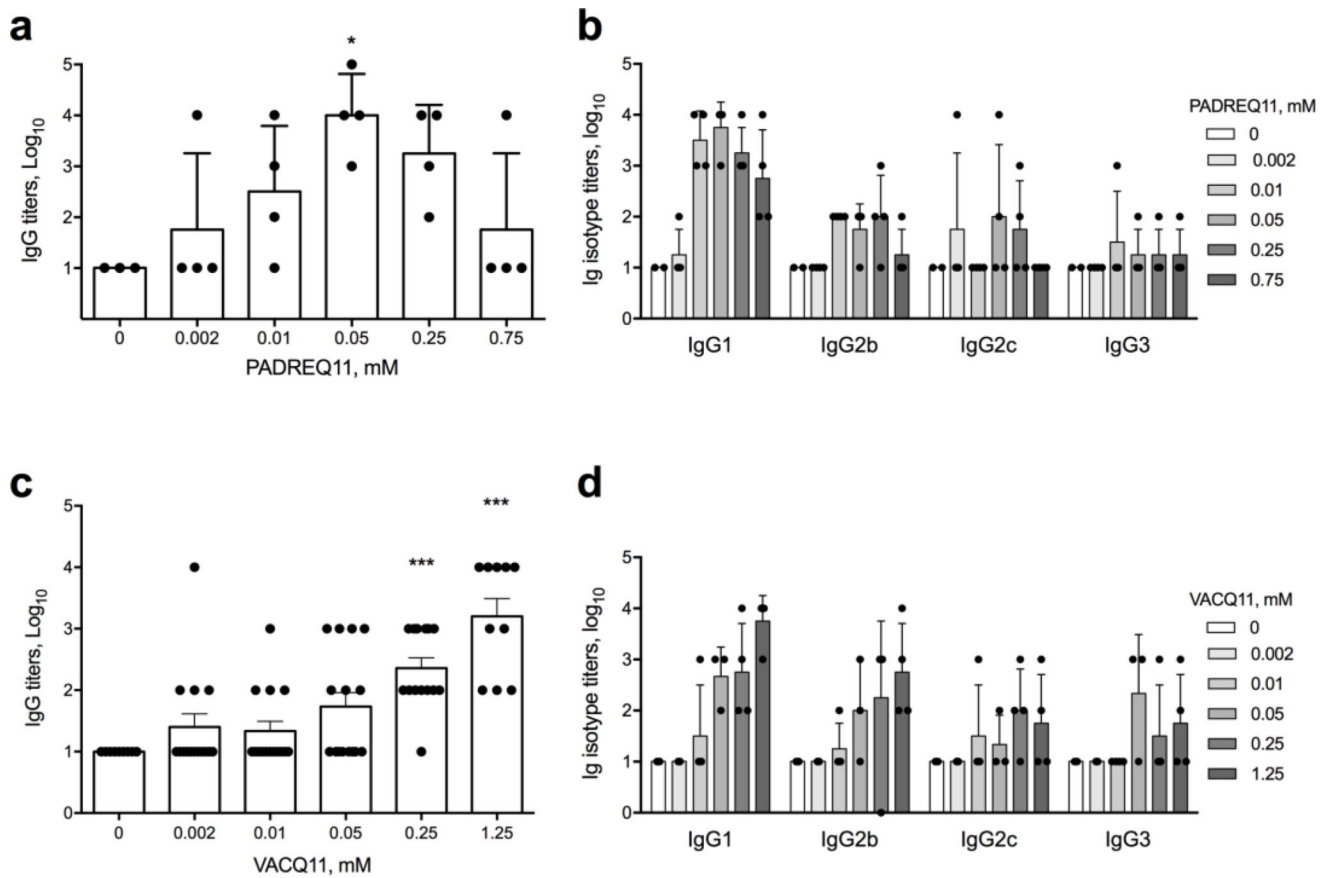


**Figure 3. The strength and phenotype of anti-TNF antibody responses can be modulated by the amount of T-cell epitopes within nanofibers**

C57BL/6 mice were immunized with peptide formulations consisting of a fixed molar ratio of 1 mM TNFQ11 peptide (B-cell epitope) and progressively increasing amounts of PADREQ11 (a, b) or VACQ11 (c, d). Total peptide in the nanofibers was brought to 2 mM with a balance of unmodified Q11 peptide. Nanofibers containing PADREQ11 showed a clear maximum in anti-TNF IgG titers at 0.05 mM PADREQ11 by ELISA probed against whole mouse TNF (a), whereas nanofibers containing VACQ11 showed progressively increasing titers with increasing T-cell epitope content (c). Immunization with PADRE-containing nanofibers elicited predominantly IgG1 antibodies (b) whereas immunization with VAC-containing nanofibers elicited IgG responses more balanced between IgG1, IgG2b, IgG2c, and IgG3 (d). In a-b, for the various PADREQ11 contents (0, 0.002, 0.01, 0.05, 0.25, and 0.75 mM) group sizes were 3, 4, 4, 4, and 4 respectively. c-d represent a combination of three independently conducted experiments, where sample sizes for the various groups were 4, 0, and 6 (0 mM); 5, 4, and 6 (0.002 mM); 4, 5, and 6 (0.01 mM); 3, 5, and 7 (0.05 mM); 4, 4, and 6 (0.25 mM); and 0, 4, and 6 (1.25 mM). Mean  $\pm$  SD is shown. Statistical significance was confirmed by ANOVA followed by Tukey's multiple comparison test. \*  $p < 0.05$ , \*\*\*  $p < 0.001$  compared to 0 mM T-cell epitope.



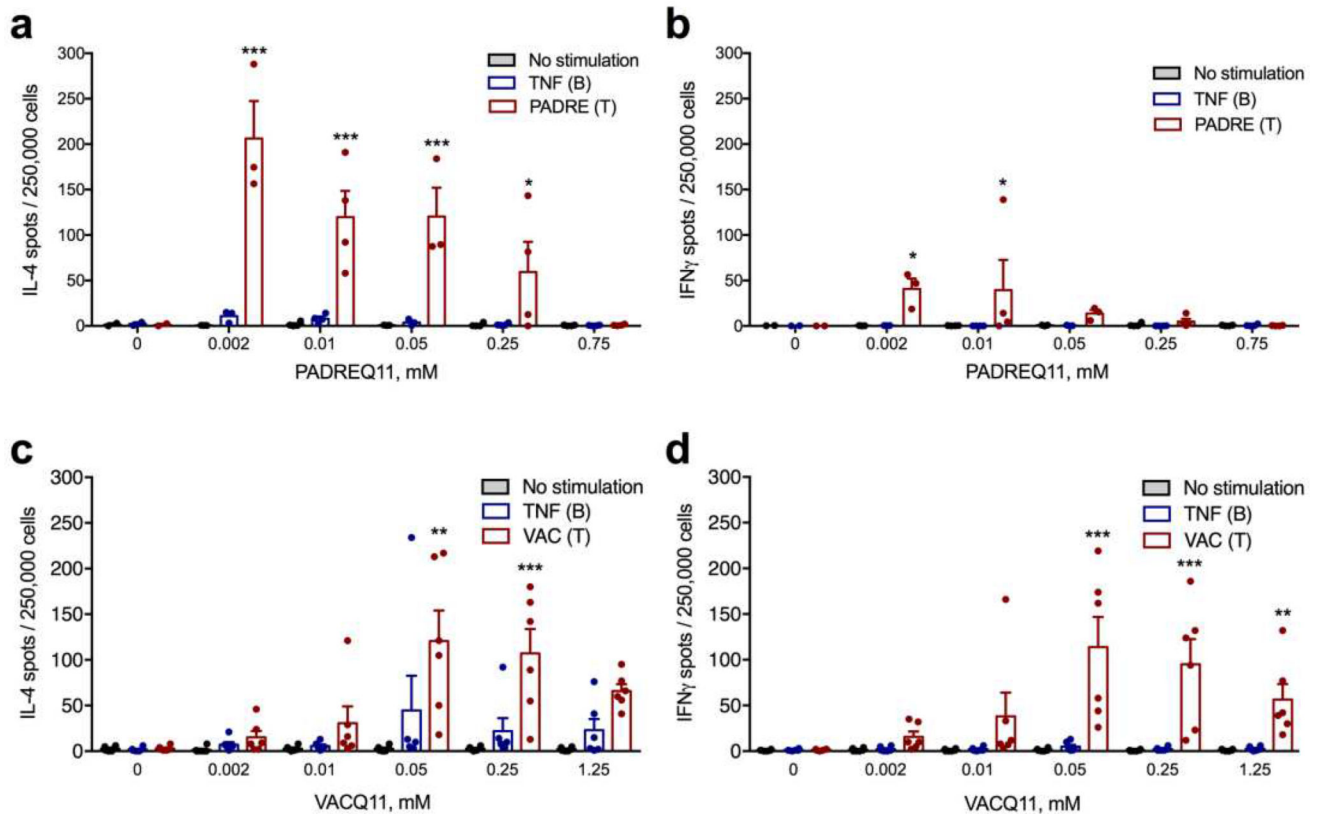


**Figure 4. Co-assembled nanofibers elicited dose-dependent T-cell responses focused on the foreign CD4<sup>+</sup> T-cell epitope, not the TNF B-cell epitope**

Cytokine-secreting cells from mice immunized with TNFQ11 combined with the indicated doses of T-cell epitope (PADREQ11 or VACQ11) were quantified *ex vivo* by ELISPOT after re-stimulation of lymph node cell suspensions with peptide TNF, peptide PADRE (a, b) or peptide VAC (c, d). In a–b, for the various PADREQ11 contents (0, 0.002, 0.01, 0.05, 0.25, and 0.75 mM) group sizes were 2, 3, 4, 3, 4, and 4 mice, respectively. c–d represent a combination of two independently conducted experiments, where sample sizes for each group were 3 mice (data in the figure shows these two experiments together, with a total sample size of 6 mice per group). Mean  $\pm$  SD is shown. Statistical significance was tested by two way ANOVA with Tukey's multiple comparison test. Significance found between T and B-cell epitope stimulation at each T-cell epitope concentration is denoted. \* $p$ <0.05, \*\* $p$ <0.01, and \*\*\* $p$ <0.001.



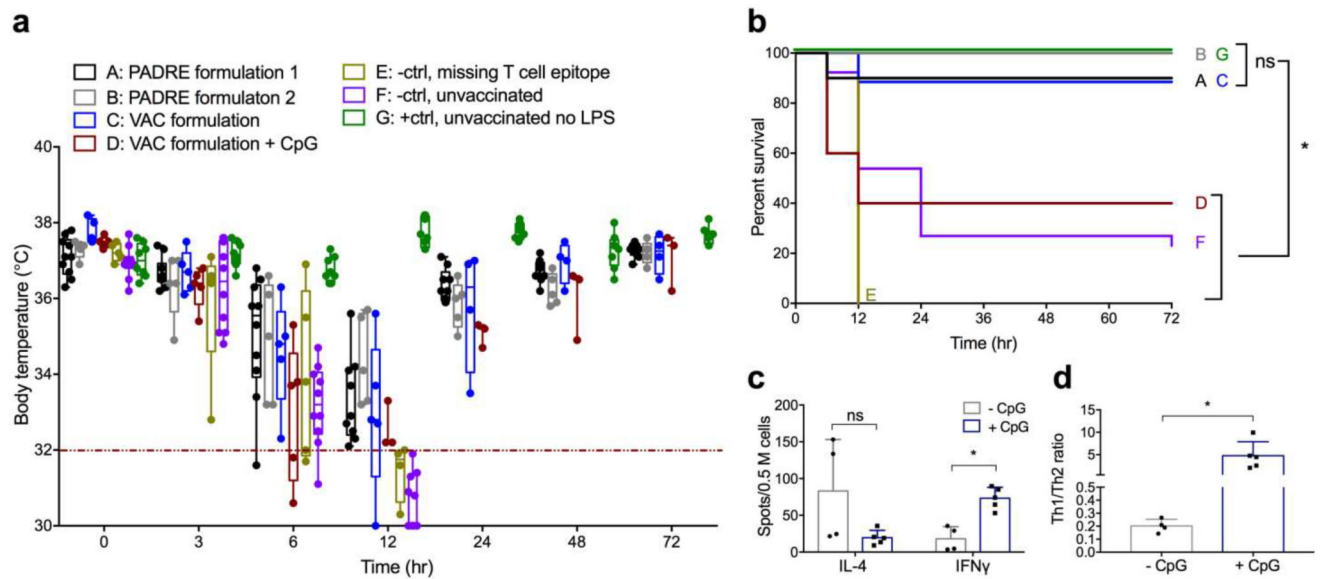


**Figure 5. Immunization with peptide nanofibers protected mice from LPS-induced inflammation**

Mice were challenged intraperitoneally with 10mg/kg LPS one week after final booster immunizations, and body temperature (a) and overall survival (b) were monitored. Humane endpoints of 32 °C (red line in a) or 20% body weight loss were employed. Group A, PADRE formulation 1: 1mM TNFQ11/0.05mM PADREQ11/0.95mM Q11; Group B, PADRE formulation 2: 0.2 mM TNFQ11/0.05 mM PADREQ11/1.75 mM Q11; Group C, VAC formulation: 1 mM TNFQ11/1.25 mM VACQ11/0.25 mM Q11; Group D, same VAC formulation as Group C, plus 10  $\mu$ g CpG; Group E, negative control, missing any T-cell epitope; Group F, negative control, unvaccinated mice receiving LPS challenge; Group G, positive control: unvaccinated mice not receiving LPS challenge. Formulations containing TNFQ11 and either T-cell epitope offered significant protection, whereas unimmunized mice, vaccinations without T-cell epitopes, and CpG-containing vaccinations had poor survival. Data points in (a) represent individual mice. Box-and-whisker plots indicate medians and 25%/75% quartiles (horizontal line and box) and max/min values (whiskers). For Group D, quartile boxes are omitted where the number of surviving mice drops below 4. Statistical comparisons of survival between all groups in (b) were made using logrank test, \* $p < 0.05$ , ns  $p > 0.05$ . Individual p-values between all groups and descriptions of experimental replicates are provided in Table S2. All experiments shown in (a) were performed at Duke University, and (b) shows overall survival curves for the mice shown in (a) plus replicate experiments performed at the University of Chicago. ELISPOT analysis (c–d) of Th1 (IFN $\gamma$ ) and Th2 (IL-4)-secreting lymph node cells from unadjuvanted nanofiber immunizations (Group C), compared with nanofibers adjuvanted with CpG (Group D). Shown are total numbers of spots (c) and ratios of IFN $\gamma$ /IL-4 spots (d). Mean  $\pm$  SD is shown. \* $p < 0.05$  by ANOVA with Tukey's multiple comparison (c) or two-tailed t-test (d).

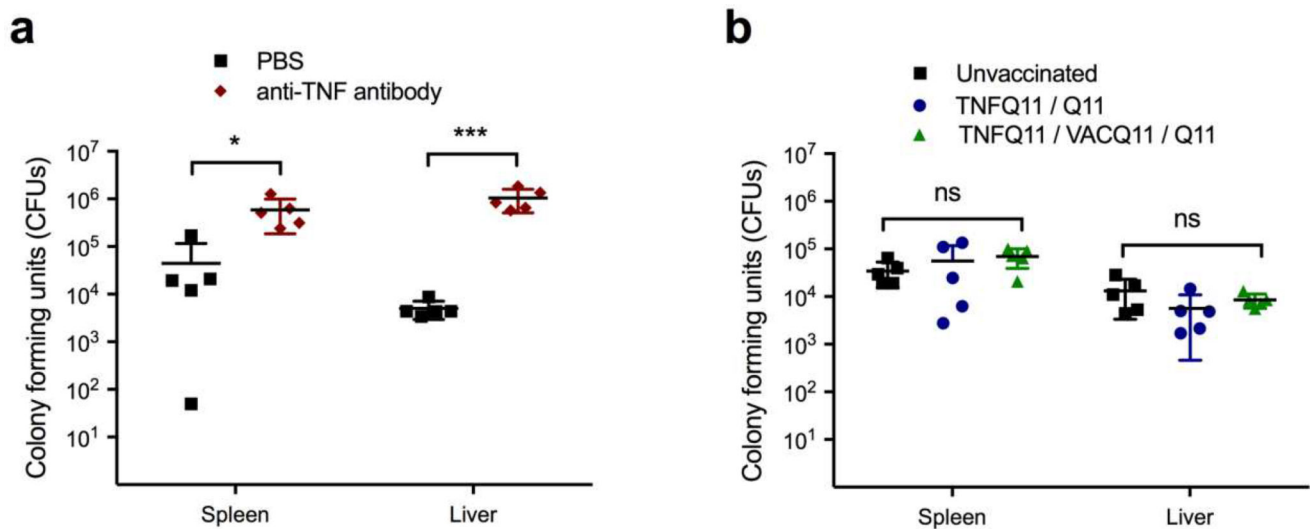


**Figure 6. Immunization with peptide assemblies did not increase susceptibility to infection by *Listeria monocytogenes***

Unimmunized mice and mice immunized with the indicated nanofiber formulations were challenged intraperitoneally with  $1 \times 10^5$  *Listeria* colony-forming units (CFU). 48 hours later, CFU were counted in the spleen and liver. Mice injected with 500  $\mu$ g of anti-TNF antibody 3h prior to intraperitoneal *Listeria* challenge had elevated *Listeria* CFU 48 hours later (a). Conversely, there were no significant differences in total CFU counts per organ between vaccinated mice, unvaccinated mice, and mice vaccinated with nanofibers lacking T-cell epitopes (b).  $n=5$  for all groups, data points represent individual mice. Mean  $\pm$  SD is shown. Statistical significance was tested using two-way ANOVA with Tukey's multiple comparison test. ns: not significant, \*  $p < 0.05$ , \*\*\* $p < 0.001$ .